Spektrum Industri
Vol. 24, No. 2, 2026, pp. 494-505
ISSN (print) 1693-6590 | ISSN (online) 2442-2630
https://journal3.uad.ac.id/index.php/spektrum/index

Manufacturing and Performance Evaluation of Ecoflex-Based Flexible Strain Sensors Reinforced with MWCNTs and Recycled Battery Carbon

Muhammad Luthfi Hakim [a,*], Ari Iswanto [b], Sigit Yatmono [a], Afri Yudantoko [c], Mohamad Shaiful Abdul Karim [d], Didik Hariyanto [a]

[a] Department of Electrical Engineering Education, Universitas Negeri Yogyakarta, Yogyakarta, 55281, Indonesia
[b] Department of Sport Education, Universitas Negeri Yogyakarta, Yogyakarta, 55281, Indonesia
[c] Department of Automotive Engineering Education, Universitas Negeri Yogyakarta, Yogyakarta, 55281, Indonesia.
[d] Faculty of Electrical and Electronics Engineering Technology, Universiti Malaysia Pahang Al-Sultan Abdullah, 26600, Pekan, Pahang, Malaysia
* Corresponding Author: luthfihakim93@uny.ac.id

ARTICLE INFO

Article history
Received August 12, 2026
Revised September 23, 2026
Accepted October 17, 2026

Keywords
Flexible strain sensor;
Ecoflex/MWCNT–RBC;
Sensitivity;
Linearity;
Durability.

ABSTRACT

Flexible strain sensors hold great potential for applications in wearable electronic devices, human motion monitoring, and rehabilitation systems. However, the development of such sensors still faces challenges in producing conductive networks that are both sensitive and stable while reducing reliance on commercial conductive materials. This study developed a flexible strain sensor (FSS) based on Ecoflex/MWCNT–RBC by utilizing recycled battery carbon (RBC) obtained from carbon rods in zinc-carbon battery waste. The RBC was separated, crushed, and sieved into a powder, then mixed with multi-walled carbon nanotubes (MWCNTs) in isopropyl alcohol using ultrasonic homogenization. The mixture was applied to a pre-cured Ecoflex layer, equipped with copper electrodes, and encapsulated using an Ecoflex layer to produce a layered sensor structure. The morphology and conductive network of the sensor were analyzed using SEM, while its electromechanical performance was evaluated through tests of sensitivity, linearity, cyclic response, response and recovery times, and durability. The sensor produced a measurement factor of 15.42 over a strain range of 0–100%, with a linearity (R^2) of 0.994. Response and recovery times were recorded at 70 ms and 70 ms, respectively, while the sensor's stability was maintained for up to 500 loading cycles at 80% strain. These results demonstrate that RBC can serve as a secondary conductive material alongside MWCNT to produce flexible, responsive, and stable strain sensors. The use of RBC also highlights the potential for reusing carbon from battery waste as a value-added functional material, while reducing reliance on commercial conductive materials in the development of flexible strain sensors.

©2026 The Author(s)
This is an open-access article under the CC–BY-SA license.

1. Introduction

Flexible strain sensors have emerged as key components in wearable electronic devices, health monitoring, electronic skin, soft robotics, and human machine interaction systems (Alfarros et al.,

2026; Gao et al., 2023; Li et al., 2025; Li et al., 2026). Unlike conventional strain sensors, which are generally rigid and have a limited deformation range, flexible strain sensors are capable of conforming to changes in the body's surface shape and detecting movements with varying degrees of deformation. The performance of these sensors is generally evaluated based on sensitivity or gauge factor (GF), strain range, linearity, response and recovery times, hysteresis, and stability under repeated loading (Hakim et al., 2025; Htwe et al., 2020). Therefore, the development of sensor materials that offer high sensitivity, good flexibility, signal stability, and a simple fabrication process remains a key focus in the field of piezoresistive sensors (Blakey-Milner, 2021; Roth, 2022).

Ecoflex is one of the elastomers widely used as a substrate for flexible strain sensors because it has a low modulus of elasticity, high strain capacity, good flexibility, and the ability to conform to the contours of the human body (del Bosque et al., 2023). However, Ecoflex is inherently insulating, so it requires the addition or coating of a conductive material to produce an electrical response to deformation. Multi-walled carbon nanotubes (MWCNT) are a promising conductive material due to their high aspect ratio, good electrical conductivity, flexibility, and ability to form conductive networks at relatively low concentrations (Sezer & Eren, 2019). When the sensor is stretched, the distance between the tubes increases and some conductive paths are broken, causing the electrical resistance to rise. Conversely, these pathways can reform when the load is released.

Several studies have demonstrated the potential of carbon networks to enhance the performance of flexible strain sensors. Long et al. developed a sensor based on carbonized corn stalks, achieving a GF of approximately 0.296 and a durability of 700 stretch-release cycles. This sensor is also capable of detecting movements of the wrist, abdomen, elbow, neck, knee, and ankle (Long et al., 2025). Bharadwaj et al. developed an MWCNT sensor with a GF of 150, a strain range of up to 427%, a response time of 100 ms, and durability of up to 100 cycles at different strains (Bharadwaj et al., 2025). Meanwhile, hybrid fabrics made of carbon black and MWCNTs have been reported to provide better conductivity because the carbon particles can fill the gaps between the MWCNT tubes (Abd et al., 2024; Wu et al., 2026). The interaction between these zero-dimensional and one-dimensional carbon materials has the potential to increase the number of conductive pathways while also amplifying the change in resistance when the fabric undergoes deformation.

On the other hand, the increasing use of electronic devices and disposable batteries has contributed to a rise in the amount of electronic waste (e-waste). In 2023, approximately 2.21 million metric tons of e-waste were reported to have been generated, but only about 20% was recycled through organized channels. This figure is projected to continue rising, reaching 74.7 million metric tons by 2030 (Abraham et al., 2019). A number of studies have utilized carbon derived from various waste materials, such as peanuts Cetin et al. (2023), used cotton fabric Chen et al. (2019), thermoset resin Wang et al. (2020), and banana peel cores Lu et al. (2024) as conductive materials in flexible strain sensors. However, the use of carbon recovered directly from zinc–carbon battery waste for such applications is still relatively limited, making it a novel aspect of this study. Used zinc-carbon batteries are a type of waste with high potential for reuse because they contain carbon materials and graphite rods that can be recovered as functional materials for flexible strain sensor applications. However, the carbon components still have the potential to be reused as functional materials. Previous research has shown that carbon materials from used zinc-carbon batteries can be recovered and processed into carbon nanoparticles or graphene-based sheets for various electronic applications (Bui et al., 2026; Wu et al., 2026).

This approach demonstrates that carbon from used batteries can be viewed not only as waste but also as a source of value-added conductive material. In this study, this material is referred to as Recycled Battery Carbon (RBC). However, the use of RBC obtained from the carbon rods of used zinc-carbon batteries as a component of a hybrid conductive network alongside MWCNTs in Ecoflex-based flexible strain sensors has not yet been extensively explored. Most previous studies have used carbon black, graphite, graphene, or commercial CNTs, while the use of recycled battery carbon has been primarily directed toward energy storage, electrochemistry, and chemical sensor applications (Abdel Sattar Kabil et al., 2026; Rawat et al., 2026).

Spektrum Industri
Vol. 24, No. 2, 2026, pp. 494–505

Furthermore, the relationship between the MWCNT–RBC composition, the morphology of the conductive network, changes in contact mechanisms and electron tunnelling, and the sensor's piezoresistive performance has not yet been comprehensively understood. MWCNTs are expected to form long, flexible main conductive pathways, while RBC particles have the potential to fill the gaps between the tubes, increase the number of contact points, and produce a conductive network that is more responsive to deformation. Based on this gap, this study developed a flexible sandwich-structured strain sensor based on Ecoflex/MWCNT–RBC by utilizing recycled carbon from zinc–carbon battery waste. The RBC was processed through the steps of separation, cleaning, drying, crushing, and sieving before being combined with MWCNT to form a hybrid conductive network. The effect of adding RBC on the sensor's morphology, electrical properties, and electromechanical performance will be evaluated through testing of sensitivity, operating range, linearity, hysteresis, response and recovery times, repeatability, and cyclic stability. In addition to introducing a new approach to organizing MWCNT conductive networks, this research offers a "waste-to-functional-material" strategy for producing economical and more sustainable flexible strain sensors for human motion monitoring applications.

2. Method

2.1. Material and Characterization

Multi-walled carbon nanotubes (MWCNTs) with diameters of 3–5 nm and lengths of 8–15 nm was obtained from a supplier in China. The flexible elastomer material used in this study was Ecoflex™ 00-30, which consists of Part A and Part B and was obtained from Smooth-On, Inc., Macungie, Pennsylvania, United States. Isopropyl alcohol (IPA), used as a dispersion medium for the conductive material, was purchased from Merck Ltd. Conductive copper tape with a width of 5 mm and a thickness of 0.1 mm was obtained from a commercial supplier and used as the sensor electrode. Recycled Battery Carbon (RBC) was obtained from the carbon rods of used AA-type zinc-carbon batteries (Fuller, 2020; Simon, 2020).

The batteries were carefully disassembled, and the carbon rods were separated from the metal components and other constituent materials. The carbon rods were then crushed using a mortar and pestle. The resulting powder was sieved using a 200-mesh sieve to ensure relatively uniform particle size. Material dispersion was performed using an ultrasonic homogenizer manufactured by Lquide Ltd., while mixing was carried out using a Thermo Scientific Cimarec heated magnetic stirrer from Thermo Fisher Scientific Ltd. Surface morphology and elemental distribution in the samples were characterized using scanning electron microscopy (SEM) equipped with energy-dispersive X-ray spectroscopy (EDS; Thermo Scientific). Electromechanical testing was performed using a testing setup adapted from a previous study (Hakim et al. 2025). During testing, changes in sensor resistance were recorded using a UNI-T UT61E+ digital multimeter manufactured by UNI-T Ltd., China.

2.2. Preparation for FSS

Fig. 1 shows the fabrication process of a flexible strain sensor based on Ecoflex/MWCNT-RBC. Recycled Battery Carbon (RBC) was obtained from carbon rods in used zinc-carbon batteries. The carbon rods were ground into powder and sieved using a 200-mesh sieve to achieve a relatively uniform particle size. MWCNT and RBC were mixed in mass ratios of 0.25 grams and 0.25 grams. The mixture was added to IPA and dispersed using a probe-type ultrasonic homogenizer for 30 minutes to reduce agglomeration and produce a homogeneous MWCNT–RBC suspension. Ecoflex Part A and Part B were mixed in separate containers using a 1:1 mass ratio. The mixture was stirred gently until homogeneous to minimize the formation of air bubbles. Next, the Ecoflex mixture was poured into a mold and leveled to form a base layer with uniform thickness. The layer was allowed to undergo a pre-curing process until its surface was stable enough to accept the conductive layer.

The MWCNT–RBC suspension was applied evenly to the surface of the Ecoflex layer using a coating method. The samples were then dried until the IPA had completely evaporated, resulting in the formation of an MWCNT–RBC conductive network. Copper tape was attached to both ends of the

conductive network to serve as electrodes. Electrical continuity was checked using a digital multimeter to ensure a stable electrical connection. The prepared Ecoflex mixture was then poured over the conductive network as an encapsulation layer. Thus, the sensor has a sandwich structure consisting of an upper Ecoflex layer, the MWCNT–RBC conductive network and copper electrodes in the middle, and a lower Ecoflex layer. The sensor then undergoes a curing process at room temperature until the Ecoflex hardens completely. After curing, the sensor is removed from the mold and cut to the dimensions of the test specimen.



Fig. 1. The process of manufacturing the Ecoflex/MWCNT-RBC sensor

2.3. Experimental setup

Electromechanical testing was conducted using a tensile testing machine equipped with a linear drive system to apply controlled strain to the flexible strain sensor, as shown in Fig. 2a. Fig. 2b and Fig. 2c show the electromechanical test setup for the sensor before and after it was stretched. Both ends of the sensor were clamped in the grips, while the copper electrodes were connected to a digital multimeter and a data acquisition system to record changes in resistance in real time. Data on resistance changes were recorded simultaneously during the loading and unloading processes at room temperature. The sensor's sensitivity was evaluated based on the relative resistance change (ΔR/R_0) with respect to the applied strain. The values of the relative resistance change and the gauge factor (GF) were calculated using Eq. (1) and Eq. (2) (Hakim et al., 2025; Hakim et al., 2025).

$$\frac{\Delta R}{R_0} = \frac{R - R_0}{R_0} \tag{1}$$

$$\mathrm{GF} = \frac{\Delta \mathrm{R}/\mathrm{R}_0}{\varepsilon} \tag{2}$$

Where $R0$ is the initial resistance of the sensor without strain, R is the resistance under strain, and ε is the applied strain. The sensor's linearity is determined through linear regression analysis between the relative change in resistance and strain, while hysteresis is evaluated based on the difference in electrical response between the loading and unloading processes. Response time and recovery time are determined by rapidly applying a strain at a specific strain level, then recording the time required for the sensor to reach the response state and return to near its initial resistance. The sensor's repeatability and stability are tested through repeated loading–unloading cycles at several specified strain levels and frequencies.

Spektrum Industri
Vol. 24, No. 2, 2026, pp. 494–505

Long-term cyclic testing was conducted to evaluate signal amplitude stability, initial resistance shift, and damage to the MWCNT–RBC conductive network following repeated deformation. The sensor's ability to detect human movement was evaluated by attaching the sensor to various body parts, such as the fingers, wrists, elbows, and knees. The sensors were connected to a portable data acquisition system to record changes in resistance during flexion and extension movements. Each test was performed at least three times to ensure the repeatability and reliability of the sensor's response.

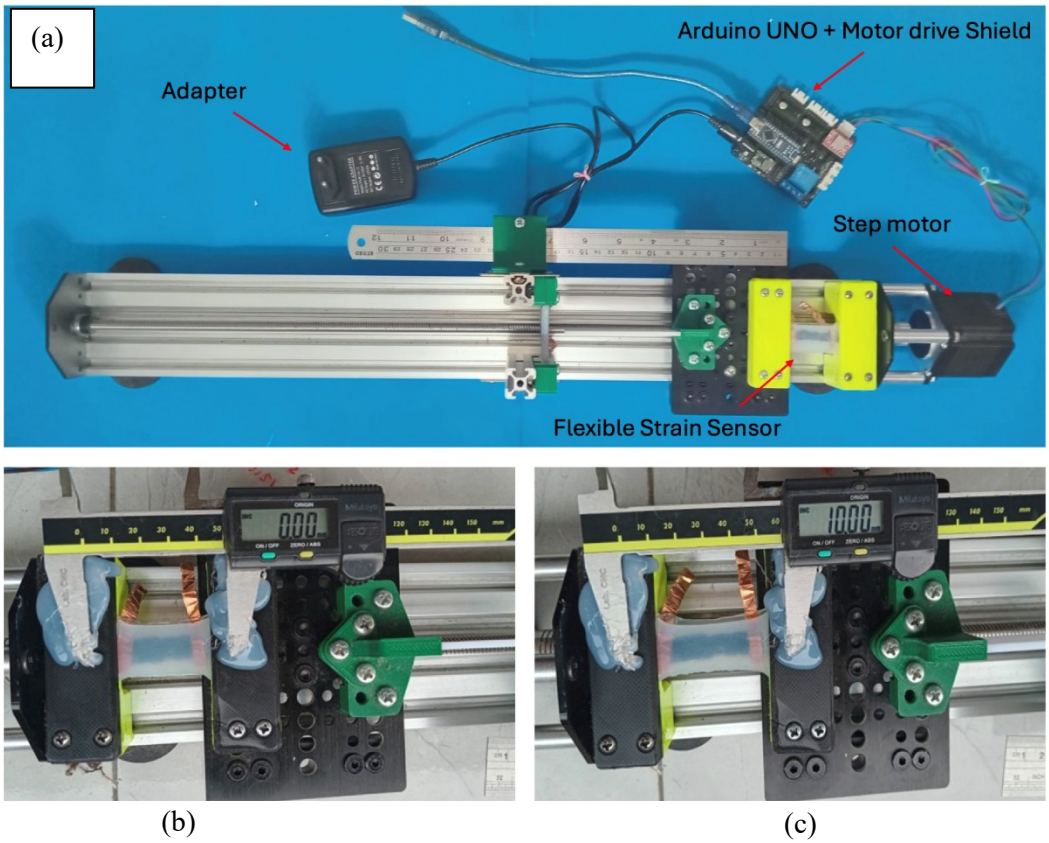


Fig. 2. (a) Electromechanical performance testing, (b) Before strain, and (c) Ater strain

3. Results and Discussion

3.1. Morphology

The cross-sectional morphology of the sensor and the MWCNT–RBC conductive network is shown in Fig. 3a. The cross-sectional image reveals a sandwich structure consisting of an upper Ecoflex layer, the MWCNT–RBC conductive network in the middle, and a lower Ecoflex layer. The conductive layer is sandwiched between the two elastomer layers, protecting it from mechanical damage and particle shedding during deformation. This structure also allows the conductive network to experience direct contact changes when the sensor is subjected to strain.

SEM observations show that MWCNTs form an interconnected tubular network, while Recycled Battery Carbon (RBC) particles are dispersed throughout the MWCNT network (Fig. 3b and Fig. 3c). MWCNTs with high aspect ratios serve as the primary conductive pathways, while RBC particles fill some of the voids between the tubes and form additional conductive contact points. The combination of these two materials results in a hybrid conductive network that is more interconnected than a network composed of only one type of carbon material. When the sensor is stretched, the distance between MWCNTs and between MWCNTs and RBC particles increases, causing some electrical contacts and electron tunnelling pathways to be (Hu et al., 2025; C. Wang et al., 2026; X. Wang et al., 2026). This condition causes an increase in the sensor's resistance. Conversely, when the strain is

released, the conductive network returns to its initial state, and most of the electrical pathways are reestablished. Therefore, the morphology of the MWCNT–RBC network plays a crucial role in determining the sensitivity, repeatability, and stability of the sensor's piezoresistive response.

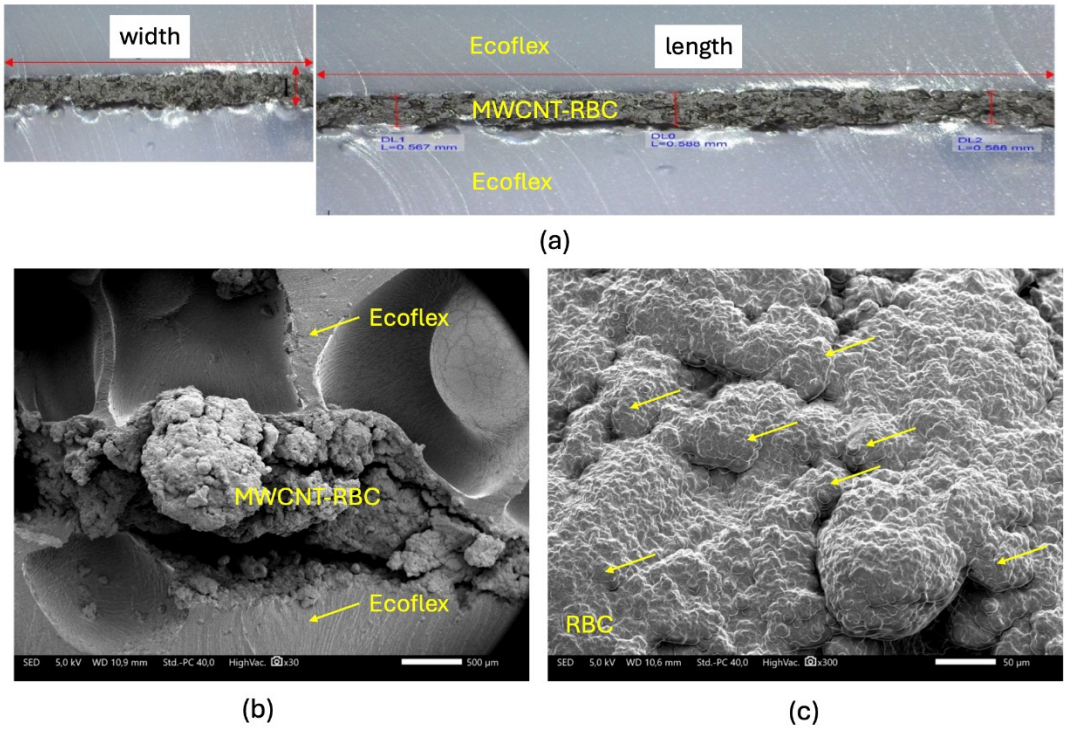


Fig. 3. (a) Cross-sectional view; (b) and (c) SEM images of the Ecoflex/MWCNT–RBC flexible strain sensor.

3.2. Sensor performance

3.2.1. Sensitivity and Linearity

Fig. 4 shows that the change in relative resistance (ΔR/R_0) increases as the strain increases. This phenomenon occurs because the distance between the MWCNTs and the RBC particles in the conductive network increases as the sensor is stretched (Khan et al., 2026; Sezer & Eren, 2019). The stretching process also causes some of the direct contacts between particles to be broken, thereby increasing the electron tunnelling resistance and the overall resistance of the sensor.

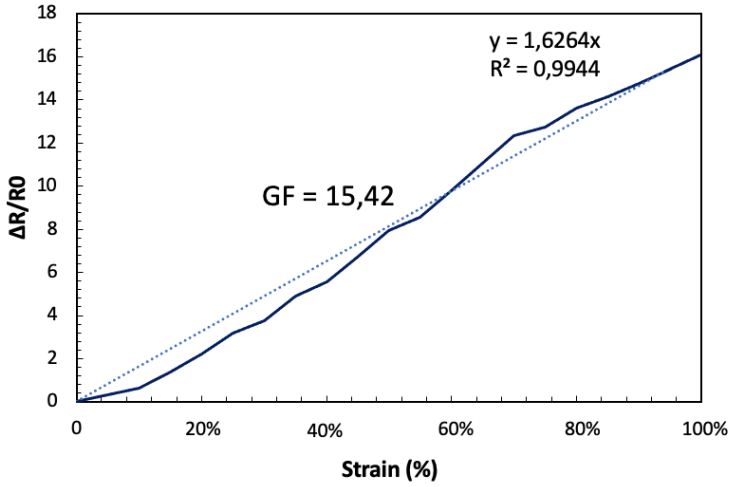


Fig. 4. Sensitivity and Linearity Values of the Ecoflex/MWCNT–RBC Sensor

Spektrum Industri
Vol. 24, No. 2, 2026, pp. 494–505

The Ecoflex/MWCNT–RBC sensor produced a GF value of 15.42 over a strain range of 0–100%. This strain ranges up to 100% was set as the test limit in this study and does not represent the absolute maximum strain that the sensor can achieve. This response is influenced by the synergistic effect between MWCNTs and RBCs in forming a conductive network. High-aspect-ratio MWCNTs play a role in forming interconnected electrical conduction pathways, while RBC particles provide additional conductive contact points between the MWCNTs. Changes in this network structure during the stretching process result in detectable changes in resistance. The sensor exhibits a nearly linear response over the 0–100% strain range, with a coefficient of determination (R^2) of 0.994. High linearity indicates that changes in sensor resistance can be used to estimate the magnitude of deformation more accurately without requiring a complex calibration model.

This linear response suggests that changes in the MWCNT–RBC network configuration occur gradually and relatively uniformly during stretching. However, deviations from the linear pattern may occur at higher strains due to increased interparticle distances, disruption of conductive pathways, the formation of microcracks, and the nonlinear deformation behavior of Ecoflex. Previous studies have reported that MWCNT@MXene sensors have an R^2 value of approximately 0.99 in the 0–100% strain range (Hakim et al., 2025). These results demonstrate that the use of hybrid conductive fillers can achieve a balance between sensitivity and linearity. Thus, the linearity of the MWCNT–RBC sensor in this study indicates that recycled carbon from batteries can contribute to the formation of a responsive and controlled conductive network.

3.3. Repeated Cyclic Response

Cyclic testing was conducted through a process of repeated loading and unloading at strain levels of 50%, 60%, 70%, and 80%, as shown in Fig. 5. The relative resistance increases when the sensor is stretched and returns to near its initial state after the load is removed. The increase in the amplitude of resistance changes at higher strains indicates the sensor's ability to distinguish between given levels of deformation. The similarity in the shape and amplitude of the signal across each cycle demonstrates that the sensor exhibits good repeatability. However, slight differences between the loading and unloading conditions may still occur due to the viscoelastic properties of Ecoflex and delays in the recovery of the conductive network. After the load is removed, the MWCNTs and RBCs require a certain amount of time to return to their initial configuration. This condition can cause slight hysteresis or a shift in the baseline resistance. Similar behavior has also been reported in MWCNT/Ecoflex sensors, where the conductive network breaks during stretching and reconnects when the load is released (Gao et al., 2023). In the sensor developed in this study, the presence of RBCs is expected to provide additional contact points to aid in the reformation of conductive pathways between the MWCNTs during the release process.

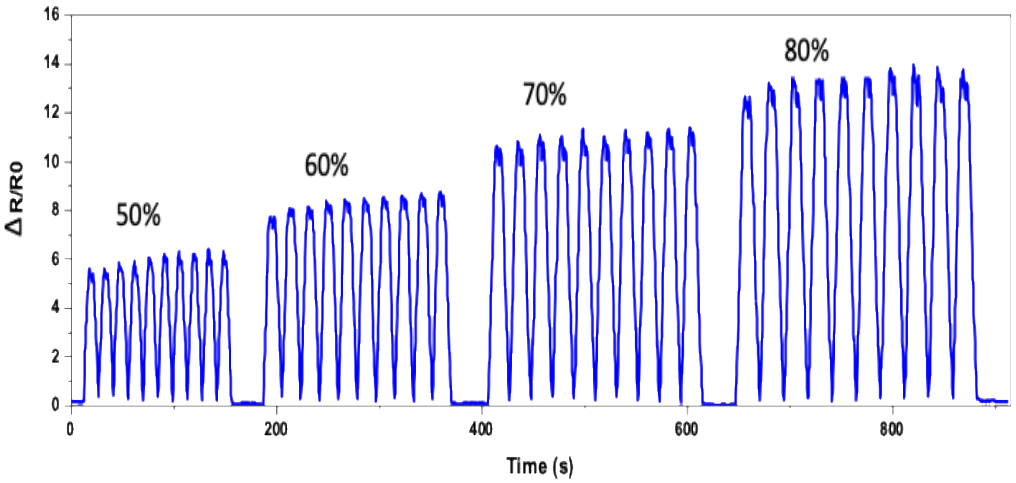


Fig. 5. Cyclic testing over 10 cycles at strains of 50%, 60%, 70%, and 80%

3.4. Response and Recovery Time

The dynamic response characteristics of the sensor are shown in Fig. 6. When a strain is suddenly applied, the sensor's resistance increases rapidly until it reaches a relatively stable state. After the load is removed, the resistance decreases and returns to near its initial value. Based on the test results, the sensor exhibits a response time of 70 ms and a recovery time of 70 ms. This response is related to rapid changes in the tunneling distance and electrical contact between the MWCNTs and the RBC. The difference between the response time and the recovery time is likely due to the viscoelastic properties of Ecoflex. The elastomer matrix requires time to recover its original shape, which in turn affects the process of reconnecting the conductive network (G. Wang et al., 2022). For comparison, Zhang et al. reported a response time of approximately 120.1 ms for a PDMS-MXene/TPU sensor (Zhang et al., 2022). Differences in response time across studies may be attributed to the thickness of the substrate and conductive layer, the type of filler, the electrode configuration, the strain level, and the data acquisition rate. Therefore, any comparison of response times must take into account the equivalence of testing conditions.

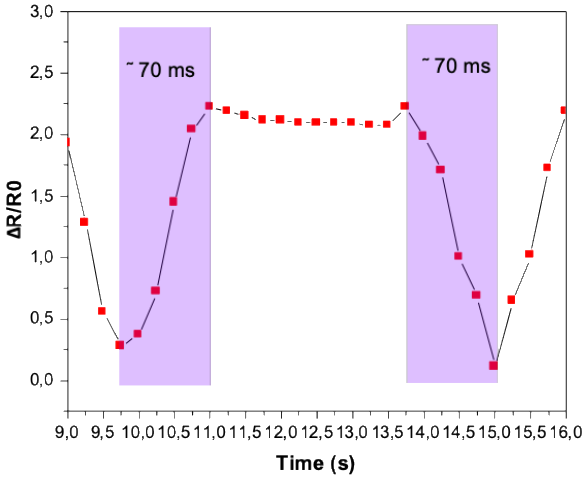


Fig. 6. Response Time of the Ecoflex/MWCNT–RBC Sensor

3.5. Durability

The sensor's durability was evaluated through 500 loading and unloading cycles at 80% strain, as shown in Fig. 7. During testing, the sensor was able to maintain a relatively stable signal shape and amplitude of resistance changes. Minor changes in both the baseline resistance and peak values may occur, but they do not cause a significant decline in sensor performance. This stability indicates that the MWCNT–RBC conductive network is capable of maintaining its integrity during repeated deformation.

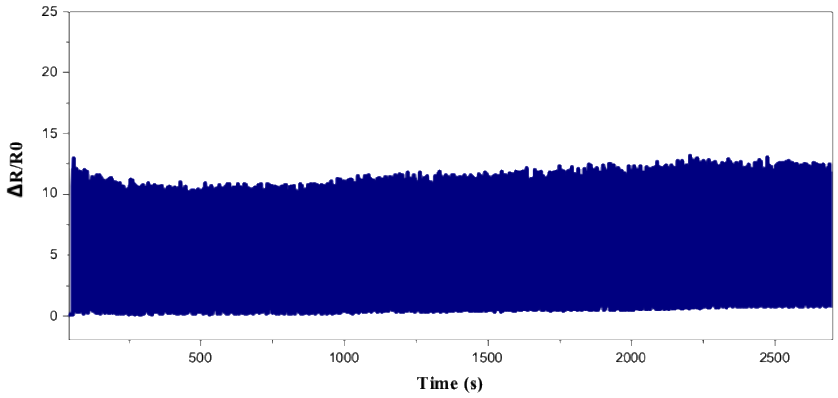


Fig. 7. Durability of the Ecoflex/MWCNT–RBC sensor

Spektrum Industri
Vol. 24, No. 2, 2026, pp. 494–505

The Ecoflex encapsulation layer serves to protect the conductive network from damage, delamination, and environmental influences. Furthermore, the interconnected MWCNT network and the presence of RBC contact points allow electrical conduction pathways to reform after the sensor is unloaded (Ghobakhloo, 2020; Khan et al., 2026). Overall, the Ecoflex/MWCNT–RBC sensor demonstrates good performance potential in terms of sensitivity, linearity, response repeatability, response speed, and stability during repeated loading. The use of RBC also provides added value through the reuse of carbon from zinc-carbon battery waste as a functional conductive material. This approach not only supports the development of flexible sensors but also contributes to waste reduction and the development of more sustainable electronic materials.

3.6. Comparison with Previous Research

This study compares the performance of the Ecoflex/MWCNT–RBC sensor with several previous studies that used comparable testing methods and evaluation parameters, including gauge factor, strain range, response time, and cyclic stability. The Ecoflex/MWCNT–RBC sensor exhibited a GF value of 15.42 over a strain range of 0–100% and a stable piezoresistive response. While some previous studies have indeed reported higher sensitivity, most still rely on commercial carbon materials, such as MWCNTs, carbon black, graphene, or other carbon-based hybrid systems. In contrast to these approaches, this study utilizes recycled battery carbon as part of the MWCNT–RBC hybrid conductive filler, so that the developed sensor not only demonstrates competitive performance but also offers added value in terms of waste utilization and material sustainability. Table 1 shows a comparison with previous studies.

Table 1. Comparison with Previous Studies

No	Materials	GF	Strain Range (%)	Time Response (ms)	Durability	Reff
1	ZnO/PEO	20.5	0~40	24	1000	(Yu et al., 2026)
2	carbon blacks/PDMS/Ecoflex	4	150	-	-	(Ge et al., 2026)
3	Laser-induced graphene (LIG)	639.51	40–60	833	2000	(Ling et al., 2026)
4	Carbon nanotube/graphene/PDMS	4.06	$80 < \varepsilon < 120$	-	1000	(T.-L. Wang et al., 2026)
5	Ecoflex/MWCNT–RBC	15.42	100	70	500	This work

4. Conclusion

This study successfully developed a flexible strain sensor (FSS) based on Ecoflex/MWCNT–RBC by utilizing carbon recovered from zinc–carbon battery waste. The combination of MWCNT and recycled battery carbon (RBC) forms an interconnected conductive network, while Ecoflex provides flexibility and protects the conductive layer during deformation. The Ecoflex/MWCNT–RBC sensor exhibits a sensitivity of 15.42 over a strain range of 0–100%, with a linearity (R^2) value of 0.994. The sensor also exhibits response and recovery times of 70 ms each and is capable of maintaining performance stability for up to 500 charge–discharge cycles at 80% strain. Overall, RBC has the potential to be used as a secondary conductive material alongside MWCNT in the fabrication of Ecoflex-based strain sensors. The use of carbon from battery waste not only produces flexible, responsive, and stable sensors but also offers a sustainable approach by converting waste into value-added functional materials. The developed sensors have the potential to be applied in wearable electronic devices, human motion monitoring, and flexible sensor-based rehabilitation systems. However, this study is still limited to testing up to 500 cycles; it has not yet evaluated the sensor's resistance to environmental conditions such as changes in temperature, humidity, and sweat, nor has it tested its performance directly on wearable devices during long-term use. Future research should increase the number of test cycles, evaluate the sensor's stability under various environmental conditions, optimize the MWCNT–RBC composition and encapsulation design, and conduct human validation to assess comfort, signal reliability, and the sensor's suitability for practical wearable device applications.

Author Contribution: Muhammad Luthfi Hakim: Conceptualization, Methodology, Investigation, Data Curation, Formal Analysis, Writing – Original Draft, Writing – Review & Editing, and Corresponding Author. Ari Iswanto: Methodology, Validation, and Investigation. Sigit Yatmono: Investigation and Data Curation. Afri Yudantoko: Formal Analysis and Visualization. Mohamad Shaiful Abdul Karim: Validation and Writing – Review & Editing. Didik Hariyanto: Supervision and Writing – Review & Editing. All authors read and approved the final manuscript.

Funding: This research received no external funding.

Acknowledgment: Extended to the Directorate of Research and Community Service at Universitas Negeri Yogyakarta, which has supported this research through the University's Flagship Research scheme for the year 2026.

Conflicts of Interest: The authors declare no conflict of interest.

Declaration of AI-Tool Usage: AI-assisted tools were used to support manuscript proofreading, verify the consistency of variables and mathematical notation, and check reference formatting. All outputs were reviewed and verified by the authors, who take full responsibility for the accuracy and integrity of the final manuscript.

References

Abd H. F. K., Hasan, M. N., Murty, G. E., Ahmad Asri, M. I., Saleh, T., & Mohamed Ali, M. S. (2024). Resistive strain sensors based on carbon black and multi-wall carbon nanotube composites. *Sensors and Actuators A: Physical*, *366*, 114960. https://doi.org/10.1016/j.sna.2023.114960

Abdel, S. K., N., Refay, N. M., Sharaf, Y. A., Ezzat, A., H., & El Nashar, R. M. (2026). Application of poly-methionine/gold nanoparticle-modified recycled battery graphite as an eco-friendly electrochemical sensor for the spasmolytic drug vincamine. *RSC Advances*, *16*(6), 5336–5352. https://doi.org/10.1039/D5RA07233F

Abraham, R., Schneider, J., & vom Brocke, J. (2019). Data governance: A conceptual framework, structured review, and research agenda. *International Journal of Information Management*, *49*, 424–438. https://doi.org/10.1016/j.ijinfomgt.2019.07.008

Alfarros, Z., Hakim, M. L., Utomo, R. S. B., Prawara, B., Kusumawanto, A., & Muflikhun, M. A. (2026). Waste (TSMP) nanocomposite for flexible strain sensors. *Sensors and Actuators A: Physical*, *400*, 117537. https://doi.org/10.1016/j.sna.2026.117537

Bharadwaj, S., Sehrawat, M., Sharma, S., Gupta, T. K., Elizabeth, I., Rani, M., & Singh, B. P. (2025). Strain detection using long-length MWCNT buckypaper-based flexible strain sensor for large strain range. *Carbon Trends*, *20*, 100525. https://doi.org/10.1016/j.cartre.2025.100525

Blakey-Milner, B. (2021). Metal additive manufacturing in aerospace: A review. *Materials and Design*, *209*. https://doi.org/10.1016/j.matdes.2021.110008

Bui, N. K., Nguyen, A.-G., Tran, N. P., Vuong, T. T. T., Dai, N. Do, Nguyen, V. N., Nguyen, P. L., & Ngo, T. (2026). Recycling carbon nanomaterials from spent battery waste for enhanced cementitious composites. *Resources, Conservation and Recycling*, *230*, 108887. https://doi.org/10.1016/j.resconrec.2026.108887

Cetin, M. S., Demirel, A. S., Toprakci, O., & Karahan Toprakci, H. A. (2023). Sustainable, bio-based conductive materials from peanut waste for flexible electronics and tunable piezoresistive strain sensors. *Materials Science and Engineering: B*, *287*, 116140. https://doi.org/10.1016/j.mseb.2022.116140

Chen, X., An, J., Cai, G., Zhang, J., Chen, W., Dong, X., Zhu, L., Tang, B., Wang, J., & Wang, X. (2019). Environmentally Friendly Flexible Strain Sensor from Waste Cotton Fabrics and Natural Rubber Latex. *Polymers*, *11*(3), 404. https://doi.org/10.3390/polym11030404

del Bosque, A., Sánchez-Romate, X. F., Gómez, A., Sánchez, M., & Ureña, A. (2023). Highly stretchable strain sensors based on graphene nanoplatelet-doped ecoflex for biomedical purposes. *Sensors and Actuators A: Physical*, *353*, 114249. https://doi.org/10.1016/j.sna.2023.114249

Fuller, A. (2020). Digital Twin: Enabling Technologies, Challenges and Open Research. *IEEE Access*, *8*, 108952–108971. https://doi.org/10.1109/ACCESS.2020.2998358

Gao, C., Liu, Y., Gu, F., Chen, Z., Su, Z., Du, H., Xu, D., Liu, K., & Xu, W. (2023). Biodegradable Ecoflex encapsulated bacterial cellulose/polypyrrole strain sensor detects motion with high sensitivity, flexibility and scalability. *Chemical Engineering Journal*, *460*, 141769. https://doi.org/10.1016/j.cej.2023.141769

Ge, Y., Ren, G., Yang, J., Shi, X., Chen, H., Fang, Q., & Yang, A. (2026). Flexible carbon blacks/PDMS/Ecoflex strain sensor for motion detection and gesture reconstruction. *Materials Letters*, *422*, 141181. https://doi.org/10.1016/j.matlet.2026.141181

Ghobakhloo, M. (2020). Industry 4.0, digitization, and opportunities for sustainability. In *Journal of Cleaner Production* (Vol. 252). https://doi.org/10.1016/j.jclepro.2019.119869

Hakim, M. L., Alfarros, Z., Herianto, H., & Muflikhun, M. A. (2025). High sensitivity flexible strain sensor for motion monitoring based on MWCNT@MXene and silicone rubber. *Scientific Reports*, *15*(1), 3741. https://doi.org/10.1038/s41598-025-88372-y

Hakim, M. L., Herianto, & Muflikhun, M. A. (2025). Next-gen strain sensors: Self-healing, ultra-sensitive, lightweight, and durable MWCNT-silicone rubber for advanced human motion tracking. *Journal of Engineering Research*, *13*(4), 3673–3686. https://doi.org/10.1016/j.jer.2024.10.009

Hakim, M. L., Muflikhun, M. A., & Herianto, H. (2025). Investigation of Electro-Mechanical Properties of SR/CNT/SR Flexible Strain Sensor Composites. *Solid State Phenomena*, *372*, 51–56. https://doi.org/10.4028/p-IsM5R3

Htwe, Y. Z. N., Mariatti, M., & Chin, S. Y. (2020). Fabrication of Graphene by Electrochemical Intercalation Method and Performance of Graphene/PVA Composites as Stretchable Strain Sensor. *Arabian Journal for Science and Engineering*, *45*(9), 7677–7689. https://doi.org/10.1007/s13369-020-04807-w

Hu, G., Zhang, Y., Chao, Y., Huang, F., Li, M., Liu, M., & Huang, W. (2025). Tunable sensitivity of strain sensor by coupling piezotronic and tunneling effects. *Nano Energy*, *145*, 111440. https://doi.org/10.1016/j.nanoen.2025.111440

Khan, A., Prathumrat, P., Likitaporn, C., Wongsalam, T., Tanalue, N., Nichakornpong, N., & Okhawilai, M. (2026). AgNP-MWCNT nanocomposites for flexible strain sensors: Comprehensive insights into green synthesis, advanced fabrication technologies, and emerging applications. *Synthetic Metals*, *316*, 118003. https://doi.org/10.1016/j.synthmet.2025.118003

Li, L., Ren, J., Han, L., Zhu, H., Aimaier, X., Fang, L., Hu, H., Zhang, B., & Zhang, R. (2025). Highly sensitive yet strain-insensitive flexible pressure sensors based on MWCNTs/TPU composites for wide-temperature-range applications. *Polymer*, *339*, 129175. https://doi.org/10.1016/j.polymer.2025.129175

Li, W., Cai, X., He, J., Liu, H., Gui, X., & Lin, S. (2026). A flexible strain sensor with high adhesion and mechanical enhancement based on PDMS/MWCNTs. *Colloids and Surfaces A: Physicochemical and Engineering Aspects*, *737*, 139752. https://doi.org/10.1016/j.colsurfa.2026.139752

Ling, J., Shen, J., Lu, S., & Hou, Y. Y. (2026). Vibration-assisted laser-induced graphene for high-performance flexible strain sensors. *Sensors and Actuators A: Physical*, *410*, 118173. https://doi.org/10.1016/j.sna.2026.118173

Long, W., Yao, Y., Ye, Y., Zhang, C., Xu, J., Zhong, D., Fu, Z., Zhang, J., Liu, X., & Xia, L. (2025). Flexible strain sensor based on carbonized corn stalk with three-dimensional network. *Industrial Crops and Products*, *225*, 120496. https://doi.org/10.1016/j.indcrop.2025.120496

Lu, Y., Zhao, X., Tian, Q., Lin, Y., Li, P., Tao, Y., Wang, Z., Ma, J., Xu, H., & Liu, Y. (2024). Hierarchical porous biomass-derived carbon with rich nitrogen doping for high-performance microwave absorption and tensile strain sensing. *Carbon*, *224*, 119083. https://doi.org/10.1016/j.carbon.2024.119083

Rawat, P., P., S. B., Patil, V. J., & P., N. G. (2026). Waste-to-sensor: Repurposing spent Li-ion battery graphite into reduced graphene oxide for electrochemical detection of ascorbic acid. *Resources, Conservation and Recycling*, *225*, 108610. https://doi.org/10.1016/j.resconrec.2025.108610

Roth, K. (2022). Towards Total Recall in Industrial Anomaly Detection. In *Proceedings of the IEEE Computer Society Conference on Computer Vision and Pattern Recognition* (Vol. 2022, pp. 14298–14308). https://doi.org/10.1109/CVPR52688.2022.01392

Sezer, H. K., & Eren, O. (2019). FDM 3D printing of MWCNT re-inforced ABS nano-composite parts with enhanced mechanical and electrical properties. *Journal of Manufacturing Processes*, *37*, 339–347. https://doi.org/10.1016/j.jmapro.2018.12.004

Simon, P. (2020). Perspectives for electrochemical capacitors and related devices. In *Nature Materials* (Vol. 19, Issue 11, pp. 1151–1163). https://doi.org/10.1038/s41563-020-0747-z

Wang, C., Xu, W., Wang, Z., Tu, H., Zhu, T., Peng, C., Shi, L., & Wu, L. (2026). Tunneling-to-contact transition enables strain-insensitive pressure sensing beyond the sensitivity–range trade-off. *Chemical Engineering Journal*, *543*, 178410. https://doi.org/10.1016/j.cej.2026.178410

Wang, G., Wang, M., Zheng, M., Yao, S., & Ebo, B. (2022). High-Sensitivity GNPs/PDMS Flexible Strain Sensor with a Microdome Array. *ACS Applied Electronic Materials*, *4*(9), 4576–4587. https://doi.org/10.1021/acsaelm.2c00782

Wang, L., Xiang, D., Zhu, W., Zhao, C., Li, Y., Han, H., Wang, P., & Wang, J. (2020). Flexible piezoresistive strain sensor with high sensitivity based on carbonised waste thermosetting resin. *Plastics, Rubber and Composites*, *49*(7), 300–306. https://doi.org/10.1080/14658011.2020.1747158

Wang, T.-L., Geng, W.-H., Wang, Y.-X., Cheng, Y.-Q., Wang, C.-D., Song, J.-M., Song, J., Zhang, D., Zhu, Q., & Geng, H.-Z. (2026). A highly sensitive carbon nanotube/graphene/PDMS composite flexible film based on multifunctional stretchable strain sensor for human activity monitoring. *Journal of Alloys and Compounds*, *1079*, 189909. https://doi.org/10.1016/j.jallcom.2026.189909

Wang, X., Liu, L., Huang, Y., Gao, Y., Dong, W., & Yao, D. (2026). A GOQD/SWCNT-PDMS flexible strain sensor enabling multi-view KFCM for railway bridge-tunnel monitoring. *Measurement*, *270*, 120803. https://doi.org/10.1016/j.measurement.2026.120803

Wu, G., Bian, P., Wang, X., Yao, M., Li, Z., Tian, J., Wu, H., Yang, J., Gu, H., Ge, Y., Ye, C., Tan, J., Liu, Q., & Wang, C. (2026). Dip-coated stretchable fabric strain sensor using a SEBS/TPU/CNC@carbon black composite. *Sensors and Actuators Reports*, *11*, 100466. https://doi.org/10.1016/j.snr.2026.100466

Wu, Y., Long, X., Li, L., Liu, L., Wu, Y., & Zeng, Z. (2026). Construction of high-mass loading dry-pressed lithium-ion battery electrodes with excellent flexibility via one-dimensional carbon nanomaterials. *Journal of Energy Storage*, *156*, 121668. https://doi.org/10.1016/j.est.2026.121668

Yu, Z., Huang, Y., Li, B., Du, X., Chen, R., Zheng, G., Wang, X., Jiang, J., & Chen, H. (2026). High-performance ZnO/PEO flexible strain sensors for accurate human physiological signal monitoring. *Sensors and Actuators A: Physical*, *410*, 118208. https://doi.org/10.1016/j.sna.2026.118208

Zhang, Z., Weng, L., Guo, K., Guan, L., Wang, X., & Wu, Z. (2022). Durable and highly sensitive flexible sensors for wearable electronic devices with PDMS-MXene/TPU composite films. *Ceramics International*, *48*(4), 4977–4985. https://doi.org/10.1016/j.ceramint.2021.11.035